Water Resources Management (2022) 36:4057–4080
https://doi.org/10.1007/s11269-022-03236-8

Impacts of Receding of the Lakes Located in the Arid and Semi-arid Areas on the Coastal Groundwater: Integrated Modeling and Experimental Study

Mahdi Motallebian[1] · Hojjat Ahmadi[1] · Amir Raoof[2] · Nick Cartwright[3]

Received: 12 March 2021 / Accepted: 24 June 2022 / Published online: 19 July 2022

Abstract
The dropping of the water level of the lakes located in the arid lands leads to salt concentration increase. In this study, a combined experimental-computational method is developed to explore the effect of seawater concentration on the elevation of groundwater table and the rate of saltwater intrusion, while the lake water level is dropping. At the laboratory tank scale, we have collected experimental data by varying the saltwater concentration by 2.0 and 2.5 times its initial value while measuring the height of the groundwater table. Our simulation has shown an unexpected increase in height of groundwater by 5.0 and 13.0% relative to the head difference at the boundaries of the domain. Also, the intrusion rate of saltwater wedge increased by 2.0 and 3.0 times, respectively. We have used the verified model for a field state and found that if density variations are neglected in simulation, the calculated groundwater level is affected more than 2 times in response to fluctuation of lake water level (relative to simulations by including the effect of fluid density changes). Based on the results density variations can counteract; even reverse, the effect of water table changes. Remarkably, our simulations have shown that despite a severe decrease in the water level of a saline lake over time, the saltwater wedge has indeed intruded further because of the substantial increase in the density of the lake water due to the rising salinity. Based on the findings, to reach a reasonable result in the study of interaction between saline water of shrinking lakes with coastal groundwater, saltwater concentration as well as saline water density in the modeling must be considered.

Keywords Coastal Aquifer · Saltwater · Density · Concentration · Lake Urmia

✉ Hojjat Ahmadi
h.ahmadi@urmia.ac.ir

Mahdi Motallebian
m.motallebian@gmail.com

Amir Raoof
a.raoof@uu.nl

Nick Cartwright
n.cartwright@griffith.edu.au

[1] Department of Water Engineering, Urmia University, Urmia, Iran

[2] Department of Earth Sciences, Utrecht University, Utrecht, The Netherlands

[3] School of Engineering and Built Environment, Griffith University, Gold Coast, Australia

1 Introduction

Water conservation and supply of freshwater are some of the main challenges in coastal areas particularly in aired and semi aired areas with high-density population due to more water consumption in domestic, industry, and agriculture (Kjelgren et al. 2000). A review of freshwater distribution confirms the amount of surface fresh water is very limited compare to groundwater in arid and semi-arid regions. Therefore, most of the water demand is supplied by the groundwater particularly in the coastal region areas where around 3.2 billion people live a coastal strip of 200 km (Singh and Tangarajan 2016).

In coastal aquifers due to the difference between fresh water and seawater density a reverse gradient is developed that leads to backward flow of saltwater below groundwater known as the intrusion. Researchers believe different parameters threaten saltwater intrusion. Abdoulhalik and Ahmed (2018) studied the saltwater upcoming in laboratory-scale coastal aquifer. The results revealed that pumping wells in aquifers with low permeability are more vulnerable to salinization than aquifers with high permeability. Yi et al. (2016) simulated the interaction between groundwater and seawater in a coastal surficial aquifer in Bohai Bay, Tianjin, China. Their findings showed that both SGD (Submarine groundwater discharge) and SWI (Seawater intrusion) occur across the sea-aquifer interface and SGD is highest in the winter and lowest in the summer. Sebben et al. (2015) classified them in different groups as the extraction of groundwater, sea-level fluctuation, coastal flooding, climate change, and land-based activities. The mentioned parameters are not independent of each other and some may directly depend upon another like sea-level rising due to climate change (Webb and Howard 2011). Saltwater intrusion makes a substantial environmental impact along with the coastal strips (Chang et al. 2011; Yuan et al. 2015; Xiao et al. 2018; Hoan et al. 2019). Gladen and Park (2016) studied impacts of intrusion result in sea-level rising in some coastal regions of Egypt, Bangladesh, Indonesia, and South Korea. Dramatically decreasing agricultural production has been reported not only by inundation but also by increasing salinity concentration of groundwater in all four studied coastal areas. A numerical study carried out by Giambastiani et al. (2007) revealed that a rising of sea level about 0.475 m leads to 800 m intrusion of saltwater toward inland. Carretero et al. (2013) studied the influence of sea-level rising on the position of the saltwater-freshwater interface. The results revealed that the position of interface would be moved up 41 times of sea level rising. In such a case, based on the conceptual intrusion model developed by Chang et al. (2011) saltwater wedge movement causes lifting of the fresh groundwater table.

Generally, all types of aquifers are recharged by precipitation. The more precipitation, the more water would flow to the groundwater and this phenomenon avoids saltwater wedge penetration into the coastal groundwater (Chang et al. 2011). Obviously, in arid and semi-arid areas rainfall seasons are limited, therefore saltwater intrusion could extend more in comparison to tropical coasts (Pettit et al. 2018).

Beyond all effective parameters that may influence the fresh water and saltwater interaction in porous media, seawater density plays the main role in the creation of interaction zone (Doulgeris and Zissis 2014). So that based on the hydrostatic distribution of pressure at the interface of saltwater and freshwater Ghyeben-Herzberg theory was configured as a function of the density of seawater. Based on the Ghyeben-Herzberg equation, 1 m displacement of groundwater table leads to moving of interface between freshwater and saltwater about 40 m at the same direction of groundwater table fluctuations in case of seawater density is around 1.025 gr/cm^3 (De Wiest 1966). By increasing the density of

seawater, the saltwater-freshwater interface lifts up which leads reduction of the thickness of groundwater.

Numerous research has been conducted about seawater density and its relation with different physical properties (McClimans 1984; Poisson et al. 1980; Millero 2000; Rodriguez and Millero 2013; Schmidt et al. 2016). The density of seawater varying from 1.020 to 1.029 kg/m3 at the surface (Garrison 2012) and increase non-linearly with the depth of the ocean (Gladkikh and Tenzer 2012). However, the saltwater density value is very high for most of the salty lakes such as Dead Sea lake, Great Salt Lake, and Urmia Lake (Karbassi et al. 2010; Oren 2018). Based on the findings of Wang et al. (2010) it is predicted that seawater in the North Atlantic will be lower, but the tropical part will be faced with getting saltier, and consequently, the density of sea will increase. Urmia Lake is a highly concentrated saltwater lake that showed a salinity increase particularly in the period of 1987 to 2017 (Karbassi et al. 2010; Farhoudi-Hafdaran and Ketabchi 2018; Jafari and Eftekhari 2013). In this period, the concentration of different salt types in the lake has significantly increased from 214 g*/l* to more than 400 g*/l*. In previous studies, the concentration of Lake Urmia in the years before 2001, less than 150 g/l, and since then, more than 300 g*/l* has been reported (Manaffar 2012; Rad et al. 2011; Farhoudi-Hafdaran and Ketabchi 2018).

Although several studies have explored the influence of rising water levels, major uncertainties have remained which hinder making future predictions especially due to salt concentration increase while receding of sea water level around the lakes located in the arid areas and subject to drying crisis. To address this problem, we have performed tank-scale experiments together with numerical simulations to explore how salt concentration affects the saltwater wedge around coastal aquifers. In this study, the effect of changes in the concentration and water level of saltwater source simultaneously on seawater intrusion in coastal aquifers has been considered and also the effect of salt water concentration on the aquifer level has been investigated. In previous studies, these issues have not been done simultaneously in the laboratory and numerically, but in this study, an attempt has been made to consider both cases in order to better understand this issue.

2 Materials and Methods

2.1 Experimental Setup

2.1.1 The Sand Tank

The experimental setup included a sand box with dimensions of 167 cm (length) × 8 cm (width) × 100 cm (height) as shown in Fig. 1a. To determine the real-time position of the saltwater-freshwater interface, measurement tapes were pasted on the sides of the sand tank. Prior to cast glass beads in the tank to make porous media, the box was filled full of water. Then glass beads were strewed uniformly in the water and were settled at the bottom. The porosity of the uniform porous medium was measured as 0.3 using the volumetric method. A homogenous porous media was created in the tank with lucid and clean sorted glass beads (0.125–0.725 mm in diameter) up to a height of 75 cm to represent the unconfined aquifer.

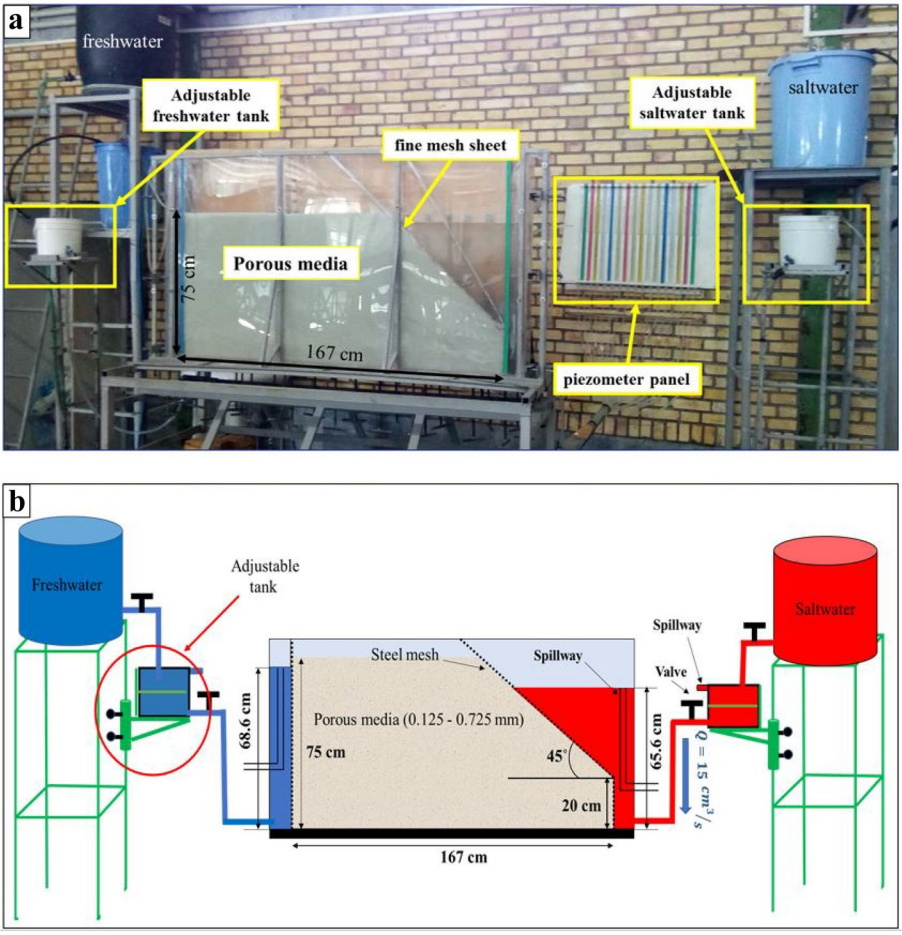

Fig. 1 **a** The experimental setup used in this study. **b** the schematic view of the setup

2.1.2 The Boundary Conditions

To assign the boundary conditions, we have used two reservoirs with adjustable water heads located at the two sides of the tank as shown in Fig. 1. The left side was connected to freshwater, and from the right side, the tank was connected to a reservoir of salt water. To create an inclined boundary at the right side of the setup with an angle of 45° and vertical in the left side in touch with fresh water, two fine stainless-steel meshes were used to keep any undesirable deformation of glass beads body. To prepare saltwater, we have collected the salt of Lake Urmia and dissolved it in tap water in a large tank. To fix the water head at each boundary, two-step water supply tanks were used at both boundaries as pointed in Fig. 1. A main big fixed position tank was used to supply saltwater and freshwater for any test. Outflow from these tanks was discharged to an adjustable tank that connected to the reservoir and so the water level in each reservoir could be easily regulated. The inlet flowrate from the main tank to the adjustable was more than that infiltrated to the porous medium therefore the extra water from these tanks was discharged using an overflow valve.

Hence, the head of water at each side reservoir was at the same level of water in adjustable thanks via a connected hose.

We considered three different salt concentrations for saltwater. For the first experiments, it was set to 35 g/l (SC_L), and for the second set to 70 g/l (SC_M), and the third to 90 g/l (SC_H). Saltwater solutions were colored as violet by dissolving 1 $g/10L$ of potassium permanganate which enabled us to distinguish it from the freshwater and to visualize the wedge zone. The density values of the colored saltwater for concentrations of 35, 70, and 90 g/l were 1.022, 1.036, and 1.046 g/cm^3, respectively. During saltwater intrusion experiments we have used a digital camera to record images every 5 min.

2.1.3 Hydraulic Properties of the Setup

To determine the permeability of the setup medium a sample of glass beads was remolded at the same void ratio of the medium in the chamber of the constant head permeability apparatus and the permeability experiments were repeated 5 times. The average value of the estimated conductivity was 0.056 cm/s. In the following to determine the dispersivity coefficient of the prepared porous medium the averaged grain size of glass beads (0.4 mm) was considered as an initial estimate for longitudinal dispersivity based on recommendations of some researchers (Tsato and Shibata 2012; GeoSlope International Ltd 2007). The traverse dispersivity is also estimated at about 1/10 of the magnitude of longitudinal dispersivity about 0.04 mm (GeoSlope International Ltd 2007; Walther et al. 2012). Furthermore, the estimated values for dispersivity were calibrated by numerical analysis with observed experimental results. Table 1 shows the properties of the material employed in the experimental setup.

2.2 Experimental Method

Before starting of the experiments, freshwater was allowed to flow from the left towards the right boundary. This flow was established using a low value of constant pressure head gradient which was held constant over time by fixing the left and right boundary heads at 68.6 cm and 65.6 cm, respectively. To keep the head fixed, tubular overflows were considered inside both left and right tanks. After establishing a steady-state flow, the saltwater was allowed to enter into the medium by opening the saltwater reservoir valve. For this purpose, the saltwater enters the tank from below and the fresh water in the reservoir exits from the intended spillway. The water at the right boundary is completely replaced by saltwater in one minute. Then, saltwater began to intrude into the tank. We let the intrusion continue until a new steady-state configuration was reached. These experiments were

Table 1 The properties of the porous medium

Parameter	Value
Porous sand medium dimensions	166 $cm \times 75\ cm \times 8\ cm$
hydraulic conductivity	48.38 m/d
porosity	0.3
longitudinal and transverse dispersion	0.4 and 0. 04 mm
Saltwater concentration	35, 70, 90 g/l
Density of saltwater	1.022, 1.036, 1.046 g/cm^3

carried out under three different saltwater concentrations of $C_L = 35$ g/l, $C_M = 70$ g/l, and $C_H = 90$ g/l. We nominated the steady-state saltwater wedge corresponding to these experiments as SC_L, SC_M and SC_H, respectively.

In all experiments, the rate of saltwater flow into the right reservoir was kept fix at a value of 15 cm^3/sec. It took almost 15 min to flow saltwater from the tank to the reservoir and refresh the saltwater in the right tank while the seepage of freshwater was discharged to the saltwater tank in the range of 0.45 to 0.75 cm^3/sec. Seepage flow of freshwater to the saltwater tank was very small in comparison to discharge from the saltwater tank, therefore the effect of freshwater in reducing salt concentration as well saltwater density was negligible.

2.3 Numerical Simulations

The SEAWAT code which belongs to the MODFLOW family to simulate variable-density flow was employed to model the steady-state and transient flow in this research. SEAWAT a finite difference based numerical model commonly has been employed by researchers to model density-dependent flow in porous media such as saltwater intrusion problems in various circumstances (Motallebian et al. 2019; Chang et al. 2018; Abdelgawad et al. 2018; Alfarrah and Walraevens 2018; Werner 2017; Gopinath et al. 2016; Javadi et al. 2015; Lu and Werner 2013; Luyun et al. 2011; Chang et al. 2011). Since the model uses finite difference method to solve the governing equation, it has some difficulties or limitations in the modelling flow problems in an irregular or complex geometry. However, for regular domain with straight boundaries such as experimental sand boxes, model gives high precision result in computing the height of saltwater wedge while may slightly overestimate length of the wedge (Ahmadi et al. 2022).

The model is capable to simulate complex problems of fluid flow and heat transfer in porous media, specifically to the analysis of saltwater intrusion. (Werner et al. 2013). The governing equation of density-dependent flow which is solved in SEAWAT has been presented by Frind (1982) as follows:

$$\frac{\partial}{\partial x}\left[\rho k_{fx}\left(\frac{\partial h_f}{\partial x}\right)\right] + \frac{\partial}{\partial y}\left[\rho k_{fy}\left(\frac{\partial h_f}{\partial y}\right)\right] + \frac{\partial}{\partial z}\left[\rho k_{fz}\left(\frac{\partial h_f}{\partial z} + \left(\frac{\rho - \rho_f}{\rho_f}\right)\frac{\partial z}{\partial z}\right)\right] = \rho S_f \frac{\partial h_f}{\partial t} + \theta \frac{\partial \rho}{\partial C}\frac{\partial C}{\partial t} - \rho_s q_s \quad (1)$$

where $\rho[ML^{-3}]$ is the density of the original aquifer water, k_{fx}, $k_{fy}.k_{fz}[LT^{-1}]$ are hydraulic conductivities of porous media in the of x, y, and z-direction respectively, $S_f[L^{-1}]$ the specific storage in term of the equivalent freshwater head, θ is the effective porosity (dimensionless), $h_f[L]$ is the equivalent head of freshwater, $\rho_s[ML^{-3}]$ the density of saltwater, $\rho_f[ML^{-3}]$ is the density of fresh water, $q_s[T^{-1}]$ is in or outlet flowrate to the aquifer and $C[ML^{-3}]$ is the concentration of saltwater.

In the case of variation of density in groundwater flow owing to the oscillation of salt concentration, redistribution of concentration accelerates fluid density dynamically that, influence the flow in porous media. Consequently, groundwater flow and salt transport in the porous media are a coupled process in this case, so that the flow Eq. (1) should be solved simultaneously with the following convection–diffusion equation in a couple system under constant effective temperature,

$$\frac{\partial C}{\partial t} = \nabla.(D.\nabla C) - \nabla.(\vartheta C) - \frac{q_s}{\theta}C_s + \sum_{k=1}^{N} R_k \quad (2)$$

where C is the salt concentration, D is defined as diffusivity that is computed as the sum of mechanical diffusion and effective diffusion. C_s is the concentration of solute that could be inflow/outflow by source/sink to model and R_k is the decay rate of solute in reaction k of N types reactions. Since in seawater the dissolved materials are different kinds of salts so in the studied time scale R_k is set zero.

One of the objects of this study was oriented to understand the consistency of experimental observed results with predictions computed by numerical imitations. The first purpose of the numerical modeling problem was to determine whether the experimental data are consistent with the predictions made by these widely used numerical models, and the second purpose was to perform simulations for a greater number of saltwater concentrations in a very relevant real field case in terms of saltwater density impacts on groundwater. In the numerical model, the porous medium with the same dimensions as the laboratory setup was introduced. Also, a structured mesh with one cm grids in space was applied (totally 167 cells in the horizontal and 75 in the vertical axis) to discretize the domain of the problem in any coordinates. For time steps, 1 min was considered.

Since water heads at both reservoirs remained constant during the tests (h_f=68.6 cm for freshwater, and h_s=65.6 cm for saltwater), the constant head boundary condition was applied for them in the numerical model as shown in Fig. 1. Besides, the concentration of saltwater at the right boundary was kept constant therefore this boundary was assigned as a constant concentration boundary. However, to assess the effect of different densities of saltwater in the studied problem three different concentrations were included as 35 g/l, 70 g/l, and 90 g/l under S1, S2 and S3 nominated experiments, respectively. The lower and upper faces of the model were marked as no-flow boundaries. Before starting the tests, the tank was in a saturated state with freshwater, in continue, by regulation of water level at both reservoirs to the mentioned levels a steady-state seepage flow was configured in the glass beads box. To2 control iterations in solving the unknown matrix, the tolerances for water head were set equal to or smaller than 10^{-4} cm and 10^{-8} g/l for concentration was accepted.

2.4 Model Accuracy

To compare the computed results against the observed results of the experimental test, specific statistical indicators were used. The accuracy of the computed data achieved by numerical analysis known as a prediction of the model (P) was quantified in comparison to the observed data (O) from experiments by using three statistical indicators (a measure of Nash–Sutcliffe (CE), root-mean-square error (RMSE) and Weighted RMSE (WRMSE)) presented as follows:

$$CE = 1 - \frac{\sum_{1}^{n} \left(O_i - P_i\right)^2}{\sum_{1}^{n} \left(O_i - \overline{O}\right)^2} \tag{3}$$

$$\mathrm{ARMSE} = \sqrt{\frac{1}{\mathrm{n}} \sum_{1}^{\mathrm{n}} \left(\mathrm{O_i} - \mathrm{P_i}\right)^2} \tag{4}$$

$$WRMSE = 0.67 \times RMSE + 0.33 \times ARMSE \tag{5}$$

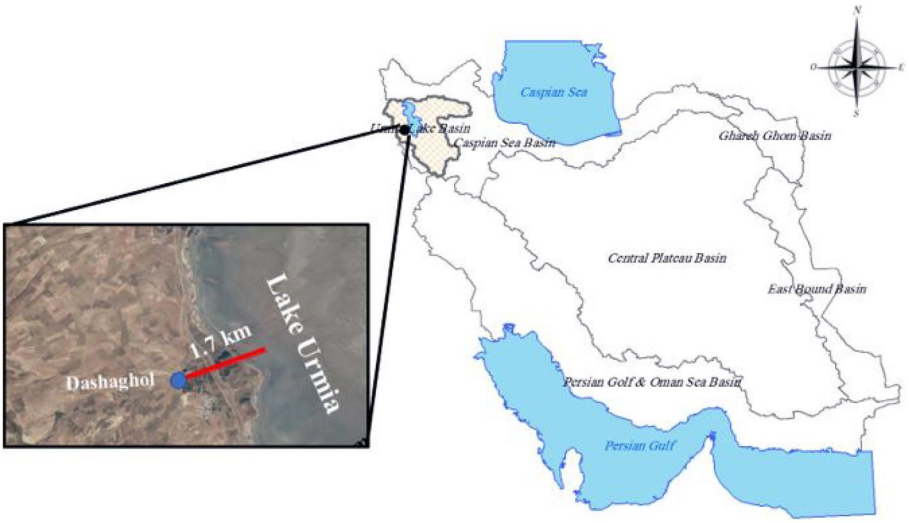

Fig. 2 Location of the Rashakan coastal aquifer in the northwest of Iran

$$\mathrm{ARMSE} = \sqrt{\frac{1}{n}\sum_{1}^{n}\left(O_i - m \times P_i\right)^2} \tag{6}$$

where O_i represent the observed position of the fresh-saltwater interface in the setup, P_i is the refer to fresh-saltwater interface computed by the model and m is the regression line slope of O_i and P_i. The theoretically desired value of RMSE, WRMSE and CE are equal to 0,0 and 1.0, respectively.

2.5 Case Study

After verification of the numerical model, we employed the SEAWAT model to simulate saltwater intrusion in a coastal aquifer adjacent to the Salt Lake Urmia (Fig. 2). Lake Urmia is a hypersaline lake located in the northwest of Iran. This lake is known as the largest saline lake in the country (Zarghami 2011) which suffers from a significant decrease in water level. The lake is surrounded by unconfined aquifers. The hydraulic and geophysical parameters of the coastal aquifer which is needed for SEAWAT are

Table 2 The parameters used in the numerical model

Parameter	Value
Hydraulic conductivity	0.9 m/day
Porosity	0.3
Longitudinal and transverse dispersion	1 and 0. 1 m
Specific yield	0.15
Length of the model	1700 m
Numerical grid size	$\Delta x = 10$ m and $\Delta z = 2$ m

presented in Table 2. The presented parameters have been estimated based on in situ investigation. As noted above, the lake has been faced with a severe drying problem and its water level has been dropped dramatically in recent years while the salt concentration raised unprecedentedly. Table 3 presents information about the water level in the lake and saltwater concentration overs years of measurement.

To modeling of the interaction between the fresh water of the adjacent aquifer with the saltwater of the lake, we have considered a cross-sectional domain with a length of 1700 m from the shore line. The left model boundary is the groundwater table of the adjacent aquifer and the right model boundary is the water level of the lake.

To investigate the impact of density changes on the groundwater table, the simulations were performed in two different conditions:

Fix Boundary Head The groundwater source, at the left boundary of the model, was considered to be infinite and at a constant level. Based on the averaged measured groundwater level at this point over 15 years it was considered at a constant level of 1282 m. In order to establish the initial steady-state conditions, the lake water level was fixed at a level of 1277.8 m. as the normal water level at the lake before the drying problem. After reaching the steady-state flow, the lake level was reduced to 1270.6 m, which is the recent year's water level in the lake.

Variable Boundary Head The groundwater source on the left of the model was assumed to be changing due to recharge into groundwater. Therefore, the water level was let to increase and/or decrease in response to the rainfall. Groundwater recharge was assumed to be 75 mm / *year*, which is approximately 30% of the average annual rainfall in the nearest meteorological station (located at the Urmia airport). As a boundary condition, the left side of the model is considered the no-flow boundary.

The simulations applying the above two conditions were carried out in three modes:

(a) **Neglecting density effects (M1 mode).** In this case, the effect of the dropping lake water level on groundwater level is studied while changes in the density of the lake water are neglected. By applying this assumption, we can find out to what extent changes in lake water level alone affects groundwater level. For this purpose, a comparison was made between the maximum level of Lake Urmia (1277.8 m) and the minimum level of Lake Urmia (1270.6). In order to establish the initial steady-state conditions, the lake level was fixed at the level of 1277.8 m above free sea level. After reaching a steady state the lake level was reduced to 1270.6 m. Saltwater concentration was assumed to be 166 g/*l* for both levels of lake water.

Table 3 Water level and its concentration in Lake Urmia (Karbassi et al. 2010; Farhoudi-Hafdaran and Ketabchi 2018; Jafari and Eftekhari 2013)

Time (Year)	Lake level (*m*)	Salt concentration (g/l)	Density ($^{g}/_{cm^3}$)
1987	1276	230	1.16
1995	1277.8	166	1.11
2004	1274	260	1.19
2008	1272	340	1.25
2012	1270.6	400	1.29

Table 4 Properties of glass bead material after calibration

Parameter	Value
hydraulic conductivity	55.3 m/d
porosity	0.22
longitudinal and transverse dispersion	0.0004 and 0.00004 m

(b) **Accounting for density effects (M2 mode).** In this case, the effect of the dropping lake water level on groundwater level is studied by considering changes in lake water density. This scenario is similar to the previous scenario, except that the effects of changing lake water concentrations by increasing and decreasing water levels are included. In order to establish the initial steady-state conditions, the lake water level was fixed at the level of 1277.8 m and the saltwater concentration was fixed at 166 g*/l*. After reaching a steady state, the lake level was reduced to 1270.6 m and the saltwater concentration was increased to a value of 400 g*/l* (see Table 3).

(c) **Intrusion rate (M3 mode).** In this part, we have explored how dropping lake water level controls the intruding or receding rates of the saltwater interface.

3 Results and Discussion

3.1 Model Calibration

To calibrate the numerical model different hydraulic conductivity of materials which has been determined in the laboratory was changed slightly till seepage flow computed by model got equivalent with experimental under steady-state freshwater flow (right reservoir with fresh water for a while). Similarly, the longitudinal and transverse dispersion for case SC_L are modified to reach best fit between saltwater wedge of model and the observed one. The final values for the calibrated parameters are summarized in Table 4. The calculated values and observed values of the position of the saltwater wedge were compared by using the Nash–Sutcliffe Efficiency (CE), the residual mean square error (RMSE) and Weighted RMSE (WRMSE) (Pandey and Pandey 2020). Table 5, presents the results of employed statistical indexes.

3.2 Experimental Results

In this section, we will first present the results of the tank experiments, and then we will proceed with the field scale results.

Table 5 Statistical indexes at SC_L experiment

	statistical indicator		
Mode	**RMSE [*cm*]**	**WRMSE [*cm*]**	**CE**
SC_L before calibration	1.03	1.11	0.988
SC_L after Calibration	0.55	0.74	0.997

3.2.1 Tank Experiments

The behavior and dynamics of saltwater intrusion under concentration change conditions were investigated in three experiments, i.e., SC_L, SC_M, and SC_H. All three experiments were performed under a single hydraulic gradient (i.e. $i = 0.018$). In the first steady-state condition SC_L, the saltwater concentration was considered 35 *g/l*. We used photos taken at 2, 4, 8, and 12 h just after the beginning of the experiment SC_L to show the Saltwater intrusion (SI) process (see Fig. 3a–d). In the first experiment, the saltwater wedge reached the steady-state after 12 h. Digital data analysis (accuracy of image analysis is ±0.01 *cm*) of the first steady-state condition (SC_L) revealed that the end of the wedge, $X_{w,}$ was almost extended to $X_w = 50$ cm and level of the crest of freshwater and saltwater interface (Z_w) was fixed at 30 cm above the model bed. (see Fig. 3e). Seepage flow in the experimental

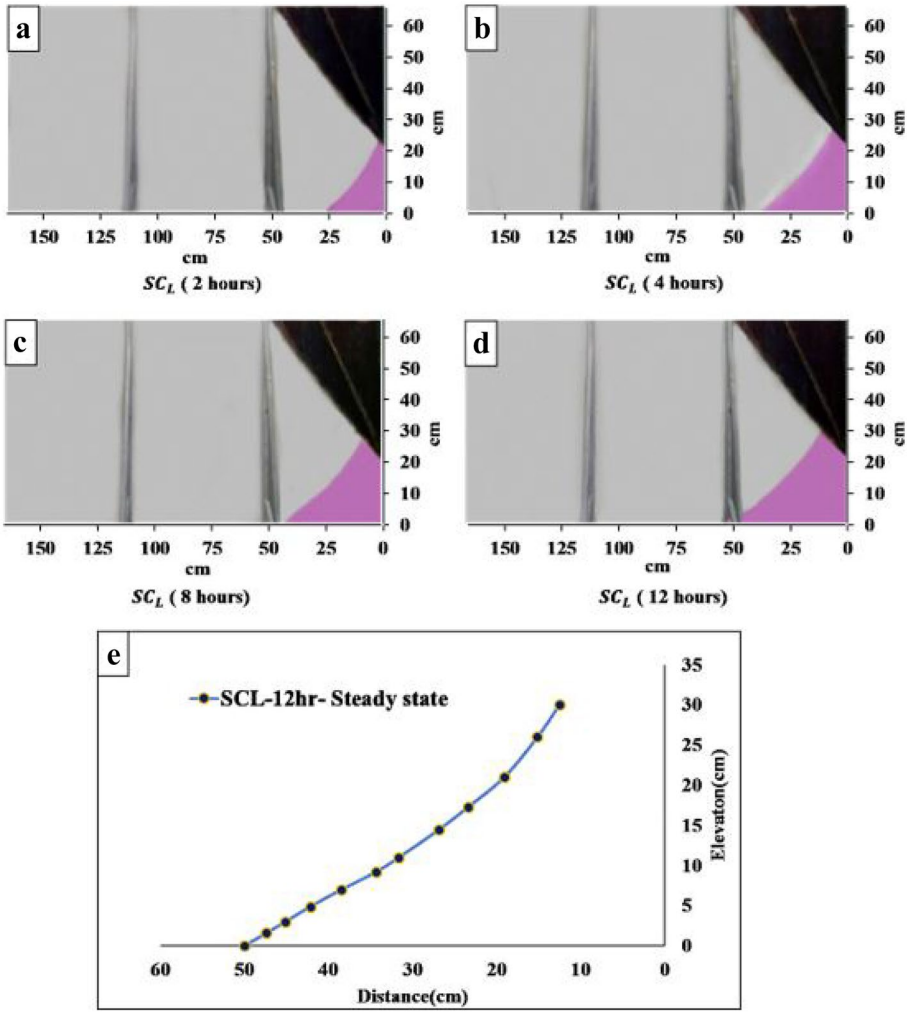

Fig. 3 **a-d** The observed salt-wedge profiles for transient experimental conditions for SC_L (i.e., C = 35 *g/l*). **e** The salt-wedge, Xw, in the steady-state conditions for SC_L

model was determined with high accuracy by measurement the discharge of inflow and outflow to reservoirs at both sides of the model. For this case, the net freshwater seepage from the left reservoir to the right was determined as 0.598 cm^3/sec.

In the second steady-state condition, SC_M, the saltwater concentration raised up to 70 g*/l*. Photos were taken at 2, 4, 12, and 25 h after the beginning of the experiment SC_M to record the SI process (see Fig. 4a–d).

Assessment of the achieved data regarding the SCM test revealed that the wedge of saltwater intrusion penetrated beneath freshwater up to 104 cm from the saltwater source tank. For the mentioned test, the crest of the wedge was lifted 44.5 cm above from the model base. The transmitted freshwater flow, in this case, was recorded at about 0.510 cm^3/sec.

The Third steady-state condition SC_H, is presented in Fig. 5a–d. The saltwater concentration to simulate this condition was 90 g/l. In the third experiment, the toe position of

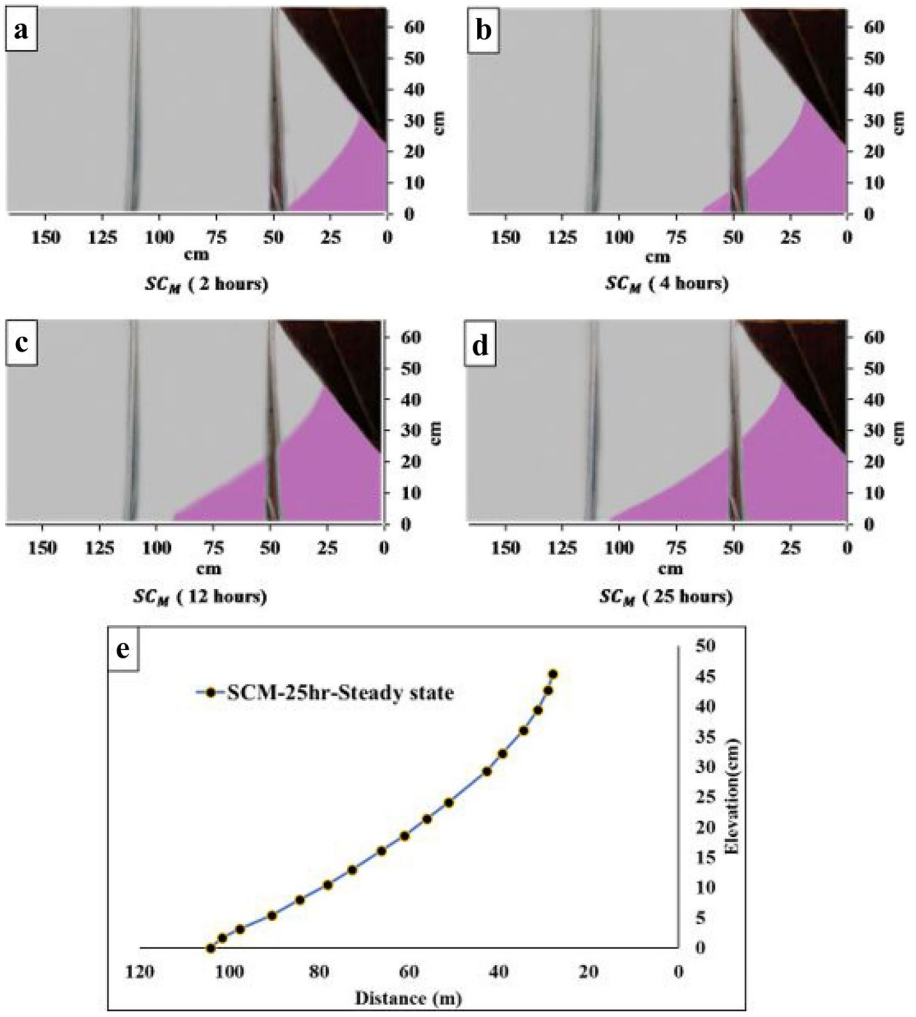

Fig. 4 **a-d** The observed salt-wedge profiles for transient experimental conditions for SC_M (i.e., C = 70 g/L). **e** the salt-wedge, X_w, profile at steady state for SC_M

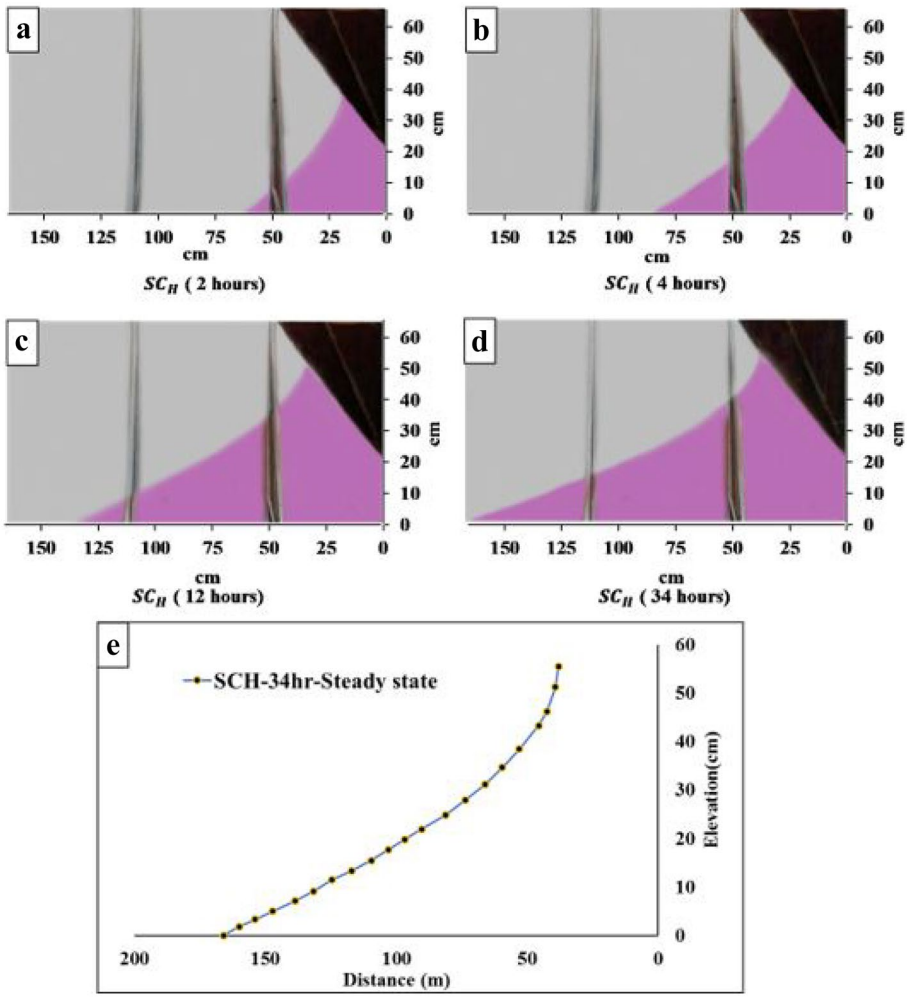

Fig. 5 **a-d** The observed salt-wedge profiles at transient experimental conditions for SC_H (i.e., C = 90 g/*l*). **e** The salt-wedge, X_w, profile at steady state for SC_H

the saltwater wedge reached the freshwater source after 25 h. At the third state of the conducted tests, the toe of the saltwater wedge was moved more and traveled 166 cm from the right boundary (X_w), the crest of the wedge raised up to an elevation of 53.2 cm (Z_w) above the model bed, simultaneously. The measured flow rate of seepage from the fresh water reservoir to the saltwater was about 0.432 cm^3/sec.

Change of saltwater concentrations in addition to changing the salt-wedge location also affects the profile of the water table. Figure 6a. shows a comparison between the tank water table at different concentrations of saltwater. The results indicate that with increasing concentration of saltwater source, groundwater table also is increased. Increasing the concentration by 2 and 2.5 times the initial concentration, the level of groundwater is increased at the laboratory scale by 0.15 and 0.4 cm respectively. In the other words, it leads to increase in height of groundwater by 5.0 and 13.0% relative to the head difference at the boundaries

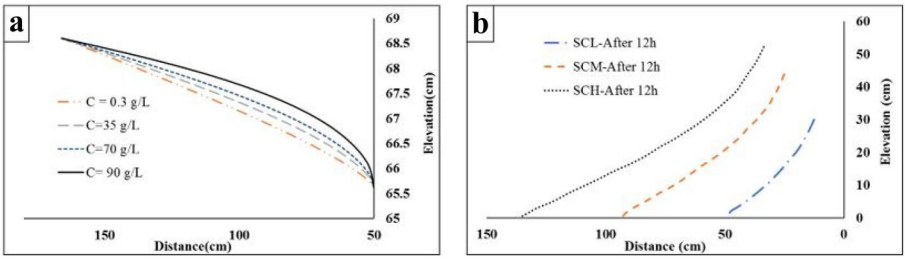

Fig. 6 **a** The water table profiles for steady-state conditions corresponding to different concentrations. **b** The salt-wedge profiles belonging to different concentrations

of the domain. Figure 6b shows the progression of saltwater wedge after 12 h for different concentrations, that it can be found by increasing the concentration by 2 and 2.5 times the initial concentration, the rate of intruding saltwater wedge is increased by 2 and 3 times. As shown in Fig. 6b as the concentration of saltwater increases, the speed of intruding the saltwater increases It can also be found from the results that the rate of flow transferred from the freshwater source to the saltwater source decreases with increasing saltwater concentration. Validation of the employed numerical model was carried out by using the collected set of seepage data and recorded digital photos.

The influence of the saltwater concentration on the position of the saltwater wedge is shown in Fig. 7. The results dictated that the toe position of the saltwater wedge has a nonlinear behaviour related to the saltwater concentration.

3.3 Numerical Simulation Results

In this section, laboratory data are compared with model predictions. At the first step, the position of the freshwater-saltwater interface at tests of SC_L and SC_M designated as steady-state intrusion tests were compared with results of numerical simulations. The results of this comparison are revealed in Fig. 8 which is shown very good agreement between observed experimental data and the model output.

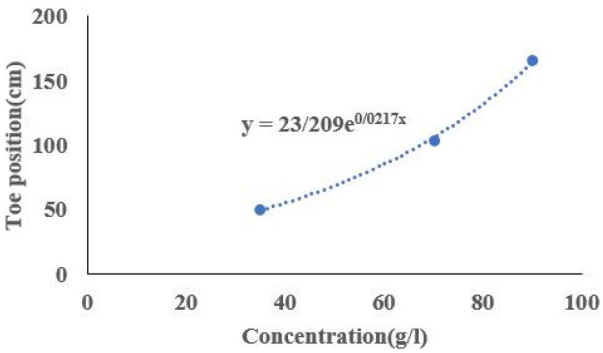

Fig. 7 Relation of concentration and toe position of saltwater wedge

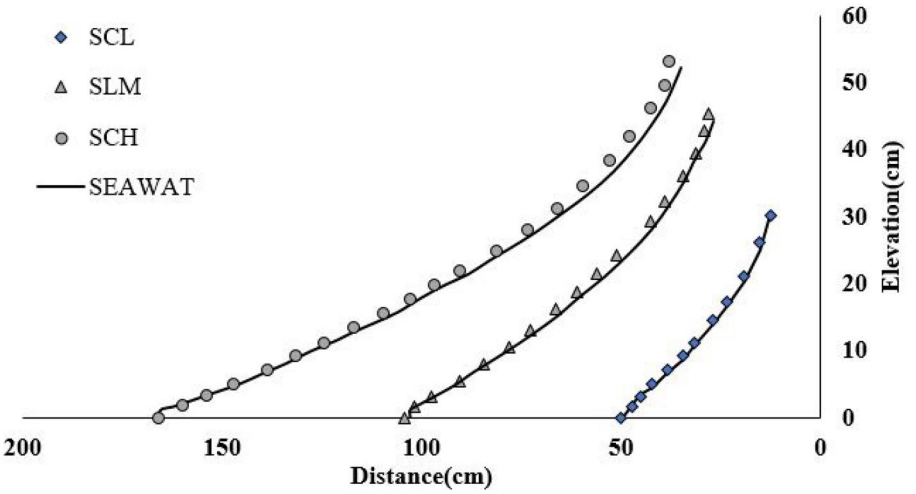

Fig. 8 Comparison of model results when steady state condition is reached against experimental data

At the second step, defined as the flux test, computed seepage flow rates were compared with the directly measured fluxes in the steady state experiments. Table 6 is allocated to results of this step and it prove acceptable accuracy of the model performance in prediction of fresh water seepage flow in the designed system.

In the third step, designated as the transient test, the numerical results are compared against the observed data of transient experiment of SC_M during unsteady transient condition before reach to steady-state. Figure 9 relates the results of this comparison, indicating a good accuracy of the model in the prediction of saltwater interface positions under transient conditions.

Figure 10 illustrates the resulting velocity field and flow patterns for different saltwater concentrations which is difficult to be measured experimentally. Figure 10 also shows that the developed SGD (submarine groundwater discharge) zones for concentrations of 0.3 (i.e. freshwater), 35, 70, and 90 g/*l*. It is clear that with increasing concentration, the rate of advancing saltwater wedge increases, and the length of the SGD zone decreases, resulting in an increase in velocity near the shore as well as a vertical flow direction, which also helps to increase the water table. Moreover, the change of velocity field alters the horizontal and vertical components of the flow field. Figure 11 shows the spatial distribution for the ratio of vertical to the horizontal velocity components corresponding to the flow fields provided in Fig. 10.

Table 6 Observed data in comparison to the model-prediction of freshwater flows

Mode	**Volumetric flow rate from freshwater resource to saltwater resource (cm^3/s)**			
	Freshwater	**SC_L**	**SC_M**	SC_H
Experimental Data	0.714	0.598	0.510	**0.432**
SEAWAT model	0.727	0.611	0.528	**0.446**

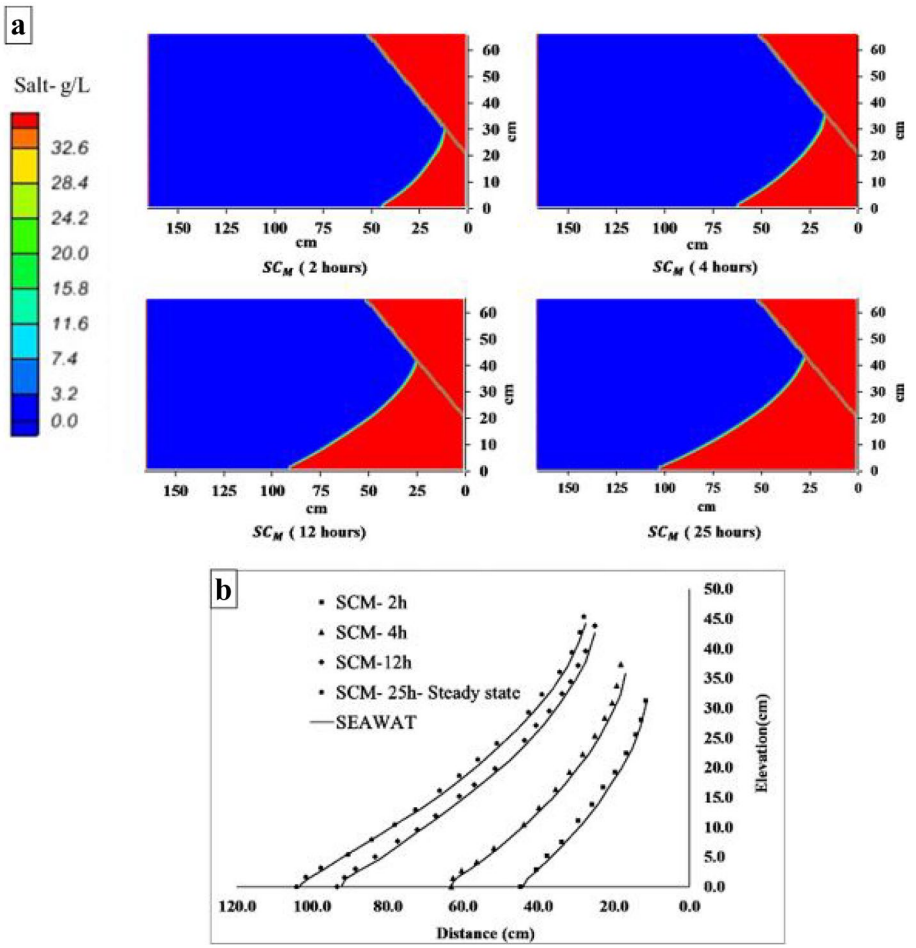

Fig. 9 **a** The model results of salt-wedge profiles at transient experimental conditions for SC_M. **b** Comparison of steady-state model for SC_M

3.4 Field-scale Results

To assess the influence of the saltwater concentration changes on the groundwater table and the interaction of freshwater and saltwater in a coastal aquifer at the field scale, the Rashakan aquifer was studied and the simulations are presented separately below.

3.4.1 Influence of the Drop-in Lake Water Level on Groundwater Table Changes Neglecting of Changes in Lake Water Density (M1)

Firstly, the effect of the drop-in lake water level on the groundwater table change was examined under condition 1 (i.e. The groundwater source on the left of the model was considered to be infinite and at a constant level). The saltwater concentration was assumed to be 166 g /*l* for both levels of lake water (1277.8 and 1270.6 m). In this case, we lowered the lake's water level by 7.2 m which was observed through the last two decades (Karbassi

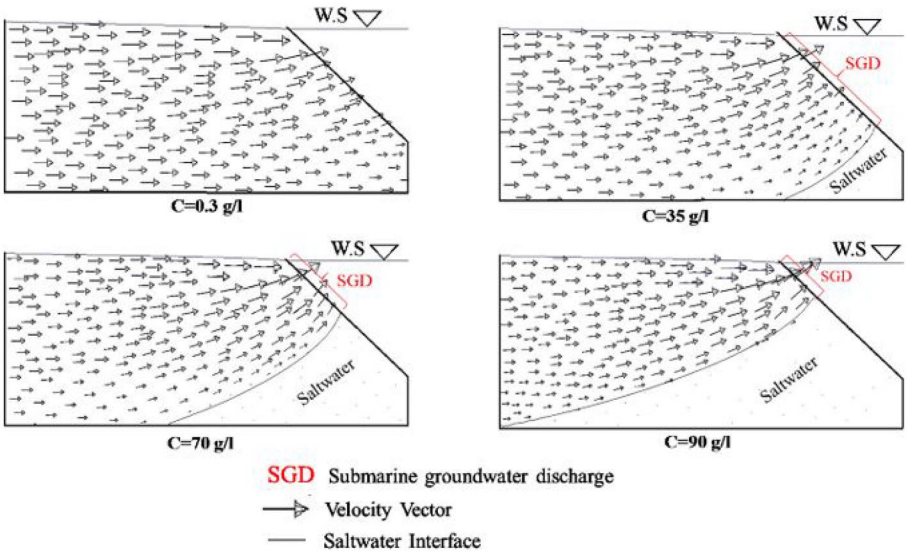

Fig. 10 The velocity filed and flow patterns under different salt concentration on the size of submarine discharge face

et al. 2010; Farhoudi-Hafdaran and Ketabchi 2018; Jafari and Eftekhari 2013). As shown in Fig. 12, the groundwater table at distances of 500, 1000, and 1500 m from Lake Urmia (the right of the model) decreased by 5, 3, and 1 m, respectively. According to the results, by moving from the shore of the lake toward the land, the impact of lake water level drop on groundwater table is lessened.

Then, the effect of the drop-in lake water level on the groundwater table change was examined under condition 2 (i.e. The groundwater source on the left of the model was assumed to be a variable level water source affected by recharging and Boundary condition for the left side of the model is considered no flow). The saltwater concentration was assumed to be 166 *g/l* for both levels of lake water (1277.8 and 1270.6 m). As shown in

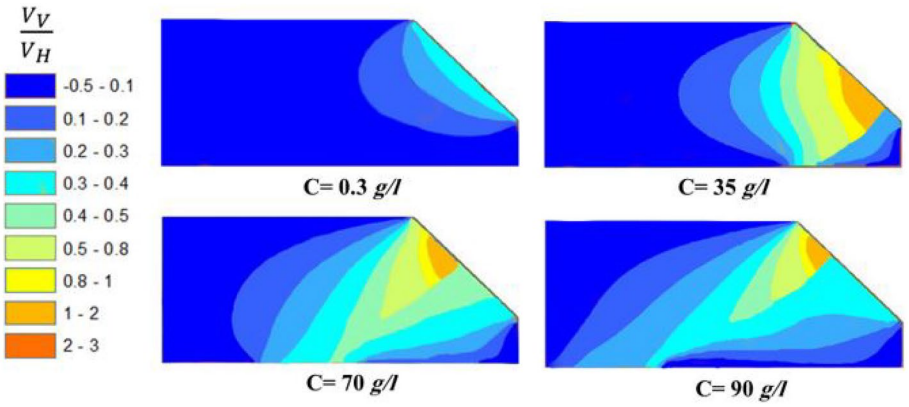

Fig. 11 The ratio of vertical to horizontal velocity showing the development of relatively strong vertical flow velocities for larger saltwater concentration values

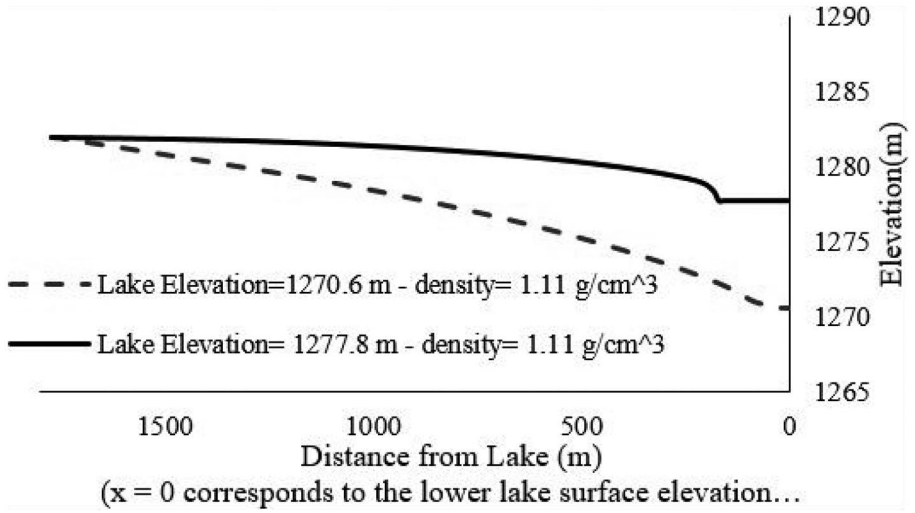

Fig. 12 Groundwater level profiles in maximum and minimum lake levels without density change effects

Fig. 13, By reducing the lake water level by 7.2 m, the groundwater level also decreased by 7.2 m. The results presented in Fig. 12 generally show that if the lake water concentration is considered to be constant, the increase and decrease in groundwater level will be equal to the increase and decrease in lake level, which is approximately equal across the aquifer.

3.4.2 Influence of the Drop-in Lake Water Level on Groundwater Table Changes

As in the previous scenario, the effect of the drop-in lake water level on the groundwater table change was examined under condition1, except that the concentration changes caused by changes in lake water volume were also considered. To establish the initial steady-state conditions, the lake water level was fixed at the level of 1277.8 m and the saltwater concentration was fixed at 166 g*/l*. After reaching steady-state, the lake level was reduced to 1270.6 m and the saltwater concentration was increased to 400 g*/l*. As shown in Fig. 14a, the groundwater table at distances of 500, 1000 and 1500 m from Lake Urmia (the right of the model) decreased by 2.8, 1.5, and 0.5 m, respectively. According to the results, by moving from the shore of the lake toward the land, the impact of lake water level drop

Fig. 13 Groundwater level profiles in maximum and minimum lake levels without density changes (variable water table on the left side of the model)

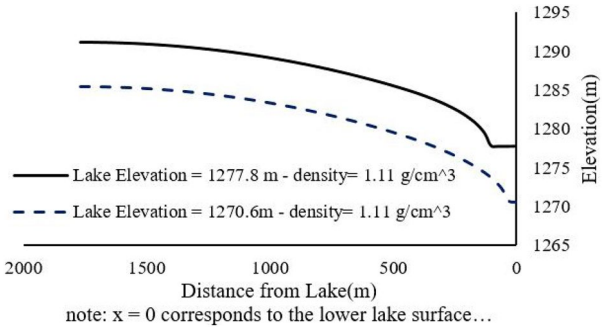

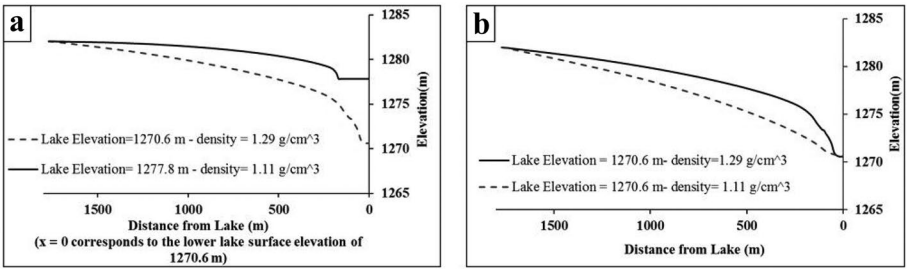

Fig. 14 Constant water table. **a** Groundwater level profiles in maximum and minimum Lake levels with density changes. **b** Comparison of Groundwater level profiles with and without the density variation when later water is at its minimum level

on groundwater table is lessened. Figure 13b compares the groundwater table profiles at the minimum water levels of Lake Urmia with and without considering density changes. The results indicate that when the density changes are neglected, the groundwater level is affected by the lake water level changes more than about 2 times than when the density changes are considered. This is because part of the pressure inserted from saltwater to the freshwater is due to the increase of concentration and density of the saltwater. When assuming constant density, this component of the saltwater pressure is neglected, and, therefore, lower heads of the water table are sufficient to counter-balance the force inserted by saltwater.

The effect of the drop-in lake water level on the groundwater table change was examined under condition 2 (cf. Sect. 2.5). In order to establish the initial steady-state conditions, the lake water level was fixed at the level of 1277.8 m and the saltwater concentration was fixed at 166 g/*l*. After reaching steady-state, the lake level was reduced to 1270.6 m and the saltwater concentration was increased to 400 g/*l*. The results presented in Fig. 15a showed that by reducing the lake level by 7.2 m, the groundwater level decreased from 1.5 to 7.2 m depending on the distance from the lake. The results indicate that the rate of decline and increase in the groundwater table is influenced by the distance from the lake. Figure 15b compares the groundwater table profiles at the minimum water levels of Lake Urmia with and without considering density changes. The results indicate that when the density changes are neglected, the groundwater level is affected by the lake water level

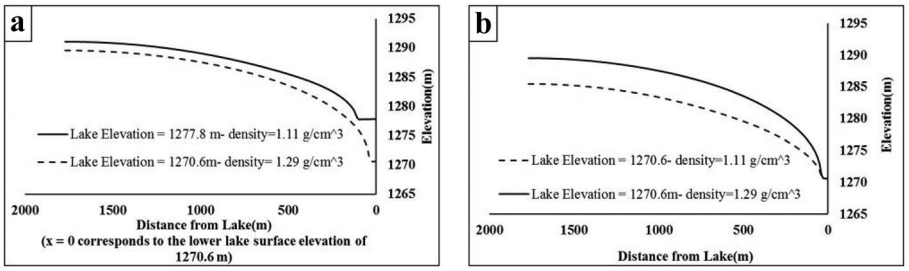

Fig. 15 Variable water table. **a** Groundwater level profiles in maximum and minimum Lake levels with density changes. **b** Comparison of Groundwater level profiles with and without the density variation in the minimum lake level

changes more than about 2 times than when the density changes are considered. Similar results were reported by Shibuo et al. (2006) regarding water level changes in Aral Sea for a 44-year period.

3.4.3 Influence of the Drop-in Lake Water Level on the Rate of the Intruding or Receding of Saltwater

The effect of the drop-in lake water level on the intruding or receding rates of the saltwater wedge was examined under condition-1(cf. Sect. 2.5) while the concentration change is neglected. In order to establish the initial steady-state conditions, the lake water level was fixed at the level of 1277.8 m, the groundwater table was fixed at the level of 1282 m and the saltwater concentration was assumed to be 166 g/L. The location wedge of saltwater is extended to 1350 m from the lake after reaching a steady state. And then the lake level was reduced to 1270.6 m without density change. At this step, the wedge of saltwater was drawn back to 607 m from the lake after reaching a steady state, which is consistent with the results of Giambastiani et al. (2007) and Carretero et al. (2013). that with the increase of the lake water level caused the advancement of saline water. Next, the effect of the drop-in lake water level on the rate of the intruding or receding of the saltwater wedge was examined under condition-1 while concentration effects are taken into account. The lake water level was fixed at the level of 1277.8 m, the groundwater table was fixed at the level of 1282 m and the saltwater concentration was assumed to be 166 g*/l*. After reaching a steady state, the lake level was reduced to 1270.6 m and the saltwater concentration was increased to 400 g*/l*. The saltwater wedge is positioned at 1770 m from the lake after reaching the steady-state condition. Figure 16a compares the saltwater wedge at the minimum water levels of Lake Urmia with and without considering density change effects.

The effect of the drop-in lake water level on the rate of the intruding or receding of the saltwater wedge was examined under condition-2 (cf. Sect. 2.5) while concentration changes were neglected. In order to establish the initial steady-state conditions, the lake water level was fixed at the level of 1277.8 m, the left side of the model the boundary conditions were not introduced as a fixed head (1282 m) and the saltwater concentration was assumed to be 166 g*/l*. The saltwater wedge is located at 390 m from the lake after reaching a steady state. And then the lake level was reduced to 1270.6 m without density change. The saltwater wedge is located at 230 m from the lake after reaching a steady state. Next, the effect of the drop-in lake water level on the rate of

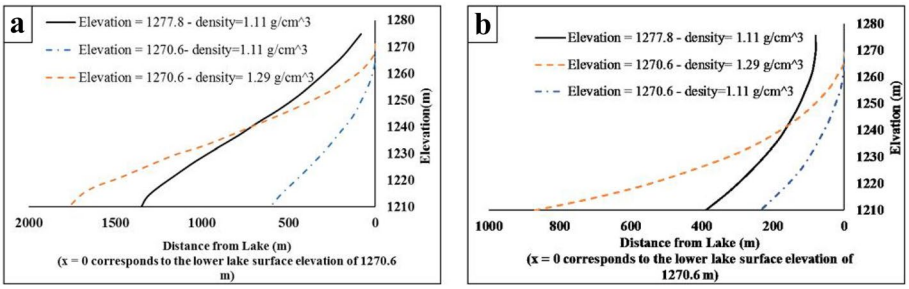

Fig. 16 Density effects. Saltwater wedge in the maximum and minimum lake levels with and without density change. **a** constant water table on the left side of the model. **b** variable water table on the left side of the model

the intruding or receding of the saltwater wedge was examined under condition-2 with considering the concentration change effects. The lake water level was fixed at the level of 1277.8 m, the left side of the model the boundary conditions were not introduced as a fixed head (1282 m) and the saltwater concentration was assumed to be 166 g/*l*. Then, the lake level was reduced to 1270.6 m and the saltwater concentration was increased to 400 g/*l*. The saltwater wedge is located at 870 m from the lake after reaching a steady state. Figure 16b compares the saltwater wedge at the minimum water levels of Lake Urmia with and without considering density changes. It can be concluded that when concentration changes and as a result of variations in density are affected, despite of decreasing the level of the lake, the saltwater wedge would be intruded unexpectedly. Otherwise, when the effect of the density changes is neglected, the saltwater wedge would be receded. Similarly, intruding of salt water in costal groundwater was reported by Vahidipour et al. (2021) around shrinking Bakhtegan-Tashk Lakes based on field monitoring. Yechieli et al. (2010) studied effect of 20 m dropping of Dead Sea water level on the coastal groundwater behaviour while the saline water density kept constant. Similar to our findings, their results showed that dropping of lake water level leads to the receding of 1 km of the saltwater edge toward the lake.

Hence, in order to study the interaction between saltwater and coastal groundwater nearby a shrinking lake, considering saltwater density variation is an essential factor that must be involved in the water management program.

4 Conclusions

The results from this study have shown that:

- The experimental results have shown that increasing saltwater concentration by 2.0 and 2.5 leads to increase in height of groundwater by 5.0 and 13.0% relative to the head difference at the boundaries of the domain., and the rate of saltwater wedge intrusion by 2.0 and 3.0 times, respectively.
- The numerical results indicated a good accuracy of the developed model in predicting the movement of the saltwater interface under transient conditions, the steady-state position of the saltwater interface, the net freshwater flow transmitted across the system.
- The results showed that the toe position of the saltwater wedge is non-linearly related to the saltwater concentration. This nonlinear behaviour was shown and discussed.
- The results of a field-scale study indicated that when the density changes are neglected during saltwater dropping, the groundwater level is affected by the lake water level changes more than about 2.0 times compared to cases where density changes are considered in flow simulation.
- The results have shown that, despite the decrease of about 7.0 m in Lake Urmia's water level, due to the substantial increase of water density, the saltwater wedge has intruded into the land. We have shown that, in the event of an increase in the water level of the lake, and consequently a decrease in water density, the saltwater wedge will recede.

Authors' Contributions Conceptualization: Hojjat Ahmadi; Methodology: Mahdi Motallebian, Hojjat Ahmadi, Nic Cartwright, Amir Raoof; Writing-Original draft preparation: Mahdi Motallebian and Hojjat Ahmadi; Writing—review editing: Amir Raoof; Supervision: Hojjat Ahmadi, Amir Raoof, Nick Cartwright.

Availability of Data and Material The data is available upon request.

Code Availability Not applicable.

Declarations

Ethics Approval Not applicable.

Consent to Participate Not applicable.

Consent for Publication Not applicable.

Conflicts of Interest/Competing Interests There is no conflict of interest.

References

Abdelgawad AM, Abdoulhalik A, Ahmed AA, Moutari S, Hamill G (2018) Transient investigation of the critical abstraction rates in coastal aquifers: Numerical and experimental study. Water Resour Manag 32(11):3563–3577

Abdoulhalik A, Ahmed AA (2018) Transient investigation of saltwater upconing in laboratory-scale coastal aquifer. Estuar Coast Shelf Sci 214:149–160

Ahmadi H, Hemmati M, Motallebian M (2022) Numerical modeling of saltwater wedge under intruding and receding conditions (Case Study: Kahriz Aquifer, Lake Urmia). Water Resour 49(2):249–258

Alfarrah N, Walraevens K (2018) Groundwater overexploitation and seawater intrusion in coastal areas of arid and semi-arid regions. Water 10(2):143

Carretero S, Rapaglia J, Bokuniewicz H, Kruse E (2013) Impact of sea-level rise on saltwater intrusion length into the coastal aquifer, Partido de La Costa, Argentina. Cont Shelf Res 61:62–70

Chang SW, Clement TP, Simpson MJ, Lee KK (2011) Does sea-level rise have an impact on saltwater intrusion? Adv Water Resour 34(10):1283–1291

Chang Y, Hu BX, Xu Z, Li X, Tong J, Chen L, Zhang H, Miao J, Liu H, Ma Z (2018) Numerical simulation of seawater intrusion to coastal aquifers and brine water/freshwater interaction in south coast of Laizhou Bay, China. J Contam Hydrol 215:1–0

De Wiest RJ (1966) On the storage coefficient and the equations of groundwater flow. J Geophys Res 71(4):1117–1122

Doulgeris C, Zissis T (2014) 3D variable density flow simulation to evaluate pumping schemes in coastal aquifers. Water Resour Manag 28:4943–4956

Farhoudi-Hafdaran R, Ketabchi H (2018) Numerical simulation of urmia lake and ajabshir coastal aquifer interaction. Iran-Water Resour Res 1:45–58

Frind EO (1982) Simulation of long-term transient density-dependent transport in groundwater. Adv Water Resour 5(2):73–88

Garrison TS (2012) Essentials of oceanography. Cengage Learning

Giambastiani BM, Antonellini M, Essink GHO, Stuurman RJ (2007) Saltwater intrusion in the unconfined coastal aquifer of Ravenna (Italy): a numerical model. J Hydrol 340(1–2):91–104

Gladen LA, Park NS (2016) Coastal groundwater development: challenges and opportunities. Groundwater assessment modeling, and management. CRC Press 534

Gladkikh V, Tenzer R (2012) A mathematical model of the global ocean saltwater density distribution. Pure Appl Geophys 169(1–2):249–257

GeoSlope International Ltd (2007) Transport modeling with CTRAN/W (Second Edition). Calgary, Alberta, Canada

Gopinath S, Srinivasamoorthy K, Saravanan K, Suma CS, Prakash R, Senthilnathan D, Chandrasekaran N, Srinivas Y, Sarma VS (2016) Modeling saline water intrusion in Nagapattinam coastal aquifers, Tamilnadu, India. Model Earth Syst Environ 2(1):2

Hoan NX, Nguyen Khoi D, Trung LD (2019) Assessing the adaptive capacity of farmers under the impact of saltwater intrusion in the Vietnamese Mekong Delta. J Environ Plan Manag 29;62(9):1619–1635
Jafari F, Eftekhari M (2013) Investigation of water exchange and penetration of the saltwater of Lake Urmia to adjoining aquifers. Water Irrig Manag (J Agric) 3:29–47
Javadi AA, Hussain M, Sherif M, Farmani R (2015) Multi-objective optimization of different management scenarios to control seawater intrusion in coastal aquifers. Water Resour Manag 29(6):1843–1857
Karbassi A, Bidhendi GN, Pejman A, Bidhendi ME (2010) Environmental impacts of desalination on the ecology of Lake Urmia. J Great Lakes Res 36(3):419–424
Kjelgren R, Rupp L, Kilgren D (2000) Water conservation in urban landscapes. HortScience 35(6):1037–1040
Lu C, Werner AD (2013) Timescales of seawater intrusion and retreat. Adv Water Resour 59:39–51
Luyun R Jr, Momii K, Nakagawa K (2011) Effects of recharge wells and flow barriers on seawater intrusion. Groundwater 49(2):239–249
Manaffar R (2012) Genetic diversity of Artemia populations in Lake Urmia. Ghent University, Iran
McClimans TA (1984) Calculating seawater surface density from temperature and speed of sound data. Deep Sea Res Part A Oceanogr Res Pap 31(11):1373–137
Millero FJ (2000) Effect of changes in the composition of seawater on the density–salinity relationship. Deep Sea Res Part I 47(8):1583–1590
Motallebian M, Ahmadi H, Raoof A, Cartwright N (2019) An alternative approach to control saltwater intrusion in coastal aquifers using a freshwater surface recharge canal. J Contam Hydrol 222:56–64
Oren A (2018) Salt lakes, climate change, and human impact: A microbiologist's perspective. Aerul si Apa. Componente ale Mediului 163–170
Pandey V, Pandey PK (2020) Calibration and ranking of Valiantzas reference evapotranspiration equations under the humid climate of northeast India. J Water Clim Chang 11(2):468–478
Pettit NE, Bayliss P, Bartolo R (2018) Dynamics of plant communities and the impact of saltwater intrusion on the floodplains of Kakadu National Park. Mar Freshw Res 69(7):1124–1133
Poisson A, Brunet C, Brun-Cottan JC (1980) Density of standard seawater solutions at atmospheric pressure. Deep Sea Res Part A Oceanogr Res Pap 27(12):1013–1028
Rad FZ, Aksoz N, Hejazi MA (2011) Effect of salinity on cell growth and β-carotene production in Dunaliella sp. isolates from Urmia Lake in northwest of Iran. Afr J Biotechnol 10(12):2282–2289
Rodriguez C, Millero FJ (2013) Modeling the density and isentropic compressibility of seawater. J Solution Chem 42(2):303–316
Schmidt H, Wolf H, Hassel E (2016) A method to measure the density of seawater accurately to the level of 10–6. Metrologia 53(2):770
Sebben ML, Werner AD, Graf T (2015) Seawater intrusion in fractured coastal aquifers: A preliminary numerical investigation using a fractured Henry problem. Adv Water Resour 85:93–108
Shibuo Y, Jarsjö J, Destouni G (2006) Bathymetry-topography effects on saltwater–fresh groundwater interactions around the shrinking Aral Sea. Water Resour Res 42(11)
Singh VP, Thangarajan M (2016) Groundwater Assessment, Modeling, and Management. Taylor and Francis Group 534
Tsato HT, Shibata M (2012) Longitudinal Dispersivity of Partially Saturated Sand Packed. Groundwater Updates 165
Vahidipour M, Raeisi E, van der Zee SE (2021) Active saltwater intrusion of shrinking Bakhtegan-Thask Lakes in South Iran threatens the freshwater resources of coastal aquifers. J Hydrol Reg Stud 34:100790. https://doi.org/10.1016/j.ejrh.2021.100790
Walther M, Delfs JO, Grundmann J, Kolditz O, Liedl R (2012) Saltwater intrusion modeling: verification and application to an agricultural coastal arid region in Oman. J Comput Appl Math 236(18):4798–4809
Wang C, Dong S, Munoz E (2010) Seawater density variations in the North Atlantic and the Atlantic meridional overturning circulation. Clim Dyn 34(7–8):953–968
Webb MD, Howard KW (2011) Modeling the transient response of saline intrusion to rising sea-levels. Groundwater 49(4):560–569
Werner AD (2017) Correction factor to account for dispersion in sharp-interface models of terrestrial freshwater lenses and active seawater intrusion. Adv Water Resour 102:45–52
Werner AD, Bakker M, Post VE, Vandenbohede A, Lu C, Ataie-Ashtiani B, Simmons CT, Barry DA (2013) Seawater intrusion processes, investigation and management: recent advances and future challenges. Adv Water Resour 51:3–26
Xiao H, Wang D, Medeiros SC, Hagen SC, Hall CR (2018) Assessing sea-level rise impact on saltwater intrusion into the root zone of a geo-typical area in coastal east-central Florida. Sci Total Environ 630:211–221

Yechieli Y, Shalev E, Wollman S, Kiro Y, Kafri U (2010) Response of the Mediterranean and Dead Sea coastal aquifers to sea level variations. Water Resour Res 46(12)
Yi L, Ma B, Liu L, Tang G, Wang T (2016) Simulation of groundwater-seawater interaction in the coastal surficial aquifer in Bohai Bay, Tianjin, China. Estuar Coast Shelf Sci 177:20–30
Yuan R, Zhu J, Wang B (2015) Impact of sea-level rise on saltwater intrusion in the Pearl River Estuary. J Coastal Res 31(2):477–487
Zarghami M (2011) Effective watershed management; case study of Urmia Lake. Iran Lake and Reservoir Management 27(1):87–94